CONF-860931--12

DE87 004998

POSTTEST EXAMINATION RESULTS OF RECENT TREAT TESTS ON METAL FUEL*

J. W. Holland, A. E. Wright, T. H. Bauer
A. J. Goldman, A. E. Klickman, and R. H. Sevy

ARGONNE NATIONAL LABORATORY
9700 South Cass Avenue
Argonne, IL 60439

International Conference on

RELIABLE FUELS FOR LIQUID METAL REACTORS

American Nuclear Society, Material Science and Technology Division

Tucson, AZ

September 7-11, 1986

* Work performed under the auspices of the U.S. Department of Energy.

Work supported by the U.S. Department of Energy, "Technology Support Program" under Contract W-31-109-Eng-38.

POSTTEST EXAMINATION RESULTS OF RECENT TREAT TESTS ON METAL FUEL

J. W. Holland, A. E. Wright, T. H. Bauer,
A. J. Goldman, A. E. Klickman, and R. H. Sevy

Argonne National Laboratory
9700 South Cass Avenue
Argonne, IL 60439

(312) 972-3079

ABSTRACT

A series of in-reactor transient tests is underway to study the characteristics of metal-alloy fuel during transient-overpower-without-scram conditions. The initial tests focused on determining the margin to cladding breach and the axial fuel motions that would mitigate the power excursion. The tests were conducted in flowing-sodium loops with uranium - 5% fissium EBR-II Mark-II driver fuel elements in the TREAT facility. Posttest examination of the tests evaluated fuel elongation in intact pins and postfailure fuel motion. Microscopic examination of the intact pins studied the nature and extent of fuel/cladding interaction, fuel melt fraction and mass distribution, and distribution of porosity. Eutectic penetration and failure of the cladding were also examined in the failed pins.

I. INTRODUCTION

A series of tests is being conducted in the Transient Reactor Test (TREAT) facility to provide information on the transient behavior of metal-alloy, fast-reactor fuel under accident conditions. The near prototypic test environment that can be created in-pile is being used to confirm inherent safety-related features of the fuel and to provide guidance to safety modeling and analysis of fuel behavior for the Integral Fast Reactor (IFR) concept. The objectives of the tests were to obtain information on two key fuel behavior characteristics under transient overpower (TOP) conditions without scram in metal-fueled fast reactors: the margin to cladding breach and the prefailure axial self-extrusion of fuel within intact cladding. Cladding breach depends upon (a) penetration of the cladding wall by formation of a low-melting-point fuel-steel alloy and (b) the internal pressure. Driving forces for prefailure fuel extrusion are fission gas, liquid bond sodium, and volatile fission products trapped within the fuel. Significant fuel extrusion prior to cladding breach would be a supporting factor in the case for benign termination of unprotected overpower events in a fast reactor.

Three tests, designated M2, M3, and M4, have been performed in Mark-III flowing sodium loops. Each test contained three uranium - 5% fissium EBR-II Mark-II driver fuel pins. These pins were suitable and available stand-ins for the U-Pu-Zr ternary alloy chosen as the reference IFR fuel. The nine pins tested included pins of 0.35, 2.4, 4.4, and 7.9 at.% burnup as well as unirradiated fuel. Each pin was contained in a separate, orificed flowtube, thereby allowing different coolant flow rates for each pin. In all three tests, the power rose exponentially from near nominal on an 8-s period. The

thermal response of each pin was monitored by nearby thermocouples, and axial extrusion was measured by the TREAT fast neutron hodoscope. Six of the pins were heated to incipient cladding breach. Three others were heated slightly beyond. Cladding failure events were monitored by thermocouples, pressure transducers, flowmeters, and the hodoscope. The power transients were rapidly terminated upon cladding breach to mitigate additional disruption of the fuel pins, which would hinder the posttest examination (PTE).

The temperatures that control cladding failure, i.e., the gas-plenum, peak mid-cladding, and peak fuel-cladding-interface temperatures, are all principally functions of the whole-pin, power-to-flow (P/F) ratio. Thus, when expressed in terms of the P/F ratio, the cladding failure thresholds measured in the tests are not only directly comparable with each other but also directly applicable to margin-to-failure assessment of pins operating in a fast reactor. Fuel performance has been described in more detail elsewhere.[1] Table 1 provides information related to the identities of the pins used in the three loop tests, their burnups, and measured and computed values pertaining to cladding failure and prefailure fuel expansion.[1] The P/F values have been normalized to the nominal steady-state reference value corresponding to 12 kW/ft axial peak power and 150 K sodium temperature rise.

Table 1. Measured and Computed Values Pertaining to Cladding Failure and Prefailure Fuel Expansion

Test	Fuel Burnup (at.%)	Max. P/F Achieved in Test	Computed Peak Plenum Pressure(a) (MPa)	Computed P/F at Onset of Fuel Melting	P/F at Half of Max. Fuel Elongation	Maximum Fuel Elongation (%)
M2	0.35	4.1	0.6-0.8	3.5	3.6	16
	4.4	4.2 (f)	7-9	2.7	3.8	(b)
	7.9	4.1 (f)	17-20	2.7	2.9	3
M3	0.35	4.1	0.6-0.8	3.5	3.7	18
	4.4	4.0	7-9	2.5	3.1	4
	7.9	3.4	17-23	2.5	2.5	4
M4	0.0	3.8	0.6-0.8	3.3	---	1
	2.4	4.1 (f)	2-6	2.3	3.2	7
	4.4	3.8	7-9	2.1	3.2	4

(a) The range shown reflects the uncertainty in the room-temperature pressure.
(b) Data are very ambiguous but seem to suggest 10-15% elongation.
(f) Cladding failure occurred in test.

Results presented in this report supplement in a valuable way information already obtained from test instrumentation and diagnostics. Location and amounts of molten fuel, as determined by PTE, checks thermal modeling. Quantitative distributions of relocated fuel mass allow the significance of observed fuel expansions to be assessed. Finally, study of the remains of fuel, cladding, and structure enables basic modeling assumptions for fuel expansion and cladding failure to be evaluated.

II. DISASSEMBLY AND NONDESTRUCTIVE EXAMINATION RESULTS

Following in-reactor operation, the three loops were transported to the Argonne Hot Fuel Examination Facility (HFEF) for initial disassembly and nondestructive examination (NDE). Loop sodium was remelted, and each test train was removed in a manner that preserved the loop for future TREAT tests. The test trains were neutron radiographed in the HFEF radiography facility to permit study of the fuel's response to the TREAT transients. Additionally, the three intact pins were extracted from the M3 test train in a manner that permitted reuse of the test train in the M4 experiment. The M3 pins remained at the HFEF to undergo NDE that included visual examination, neutron radiography, isotopic gamma scanning, contact profilometry, and plenum-gas analysis.

The M2 and M4 test trains, each containing failed fuel pins, were transported to the Alpha Gamma Hot Cell Facility (AGHCF) where they were disassembled to retrieve the intact pins and to remove the flowtubes containing failed pins. The one intact pin from M2 and two from M4 were returned to the HFEF to undergo NDE as did the M3 pins. The fuel and cladding remains from the failed M2 and M4 pins were epoxy-stabilized within their intact flowtubes to preserve their posttest configurations during subsequent examinations.

Neutron radiographs of the individual intact pins, shown in Fig. 1, provide evidence of the prefailure fuel elongation experienced during the tests. Total prefailure elongation was more than 17% (relative to the pretest fuel length) in the 0.35 at.% burnup fuel. Prefailure fuel elongation in the fuel pins that failed has been reported to be about 7% for the 2.4 at.% burnup pin, and only about 4% for the 4.4 and 7.9 at.% burnup pins.[1] The propensity for fuel elongation increases after extensive fuel melting occurs; bubble expansion to equilibrium is rapid, and coalescence of small fission gas bubbles is likely since surface tension no longer constrains the expansion. The amount of axial extrusion is effected principally by allowing the volume of fission gas dissolved in the molten fuel to expand to the pressure of the pin plenum.[1] Therefore, high burnup pins, which contain high pin plenum pressures, would be expected to experience less axial fuel extrusion than pins with lower burnups and plenum pressures.

The extent of postfailure fuel motion from the three failed pins in tests M2 and M4 is illustrated in the neutron radiographs shown in Fig. 1. All three pins failed near the top of the active fuel column where the cladding was the hottest. Massive ejection of 30-50% of the fuel occurred in all cases through a localized cladding breach. Nearly all of the ejected fuel monotonically dispersed upward beyond the initial fuel zone. In the 2.4 at.% burnup pin, the ejected fuel originated from the upper 3/4 of the fuel column. More than half of the fuel initially in the top half of the fuel

column left the cladding, and there was significant density reduction below the midplane. Within the 4.4 at.% burnup pin, voiding began in the lower 2/3 of the original fuel zone, and the bottom half of the fuel column had less than half of its initial amount of fuel when fuel motion stopped. Within the 7.9 at.% burnup pin, fuel voiding in the lower half of the fuel column was nearly complete. A likely cause of the rapid fuel dispersal upon cladding failure is sudden flashing of sodium, logged within the fuel porosity, as the pin rapidly depressurizes. The greater disruption in the high burnup pin correlates with the greater depressurization.

III. MICROSCOPIC EXAMINATION RESULTS

The intact pins from M2 and M3 and the two flowtubes containing failed pins from M2 have been sectioned to permit study of the location and nature of cladding breach sites, fuel/cladding interaction, fuel mass distribution, nature and distribution of porosity within intact fuel pins, and fuel melt fractions. The study included detailed sectioning of fuel pins and flowtubes, length and mass measurements of fuel-pin segments, metallographic examination of representative specimens, and electron-beam analysis to evaluate phase composition and morphology. Microscopic examination of the M4 pins is currently underway.

A. Cladding Breaches in Test M2.

Neutron radiographs of the M2 test train indicated that the medium- and high-burnup pins failed at the cladding "dimples." (The dimples are crimps in the cladding, located 1.3 cm above the as-fabricated top of the fuel column, to prevent upward fuel relocation during preirradiation handling.) The cladding of the high-burnup pin failed by a ballooning type rupture of 1-cm length. The medium-burnup pin failed by what appeared in the radiographs to be a transverse break in the cladding; the cladding did not balloon before failure as did the high-burnup pin. No other failure sites were observed in the radiographs or discovered during the sectioning of the pins. Fig. 2 contains two low-magnification micrographs of the medium- and high-burnup pin failure sites. The longitudinal sections show the pins within their respective flowtubes. Fuel/steel material coated much of the inner and outer surfaces of the fuel-pin cladding and much of the inner surfaces of the flowtubes, adjacent to the breaches. Destructive examination of the pins provided evidence that what appeared in the radiographs as solid chunks of fuel dispersed axially throughout the original fuel zones of the failed pins were in fact hollow shells of uranium-rich material cast in varying thicknesses against the inside of the cladding. Both pins were essentially hollow as shown in Fig. 2. Cladding near the failure site of the medium-burnup pin, shown in Fig. 2(a), sustained significant damage due to penetration by fuel/cladding eutectic, and the weakened cladding failed as a result of the moderate pin plenum-gas pressure.

Figure 2(b) illustrates the ballooning of the cladding that was observed at the high-burnup-pin breach site. Failure was likely the result of high plenum-gas pressure. The breach site at the top of the fuel, shown in Fig. 3, was exposed by making a transverse cut through the longitudinal metallography specimen at the bottom of the bulge. Fig. 3(a) shows the breach at that elevation and fuel/steel material that exited the breach cast against the fuel-pin spacer wire and flowtube. The micrograph in Fig. 3(b) was

produced after repeated grinding upward into the cladding bulge where the breach is much wider than at the elevation shown in Fig. 3(a). One of the cladding "dimples" can be seen at 8 o'clock in Fig. 3(b). The region between the "dimple" and breach is shown at higher magnification in Fig. 3(c). A low-melting fuel/steel material, formed by the interaction of cladding with fuel, moved to the breach site as a result of the fuel expulsion and froze against the inner and outer surfaces of the thinned cladding wall. Computations indicate that the fuel/cladding interface temperature was too low at the time of failure for significant thinning to occur prior to cladding breach.

B. Fuel/Cladding Interaction.

U-5Fs fuel and Type 316 stainless steel cladding are known to form low-melting phases at temperatures well below the stainless steel melting point. Failure of medium-burnup pins was expected to be controlled by cladding thinning by fuel/steel eutectic formation and hydrostatic loading by the pin plenum pressure. Failure of pins of very low burnup was predicted after the cladding became nearly completely penetrated by eutectic formation. On the other hand, the peak plenum pressure in the 7.9 at.% burnup pins was so high that failure was computed to occur before significant thinning of the cladding took place.

Metallographic examination of the failed pins from M2 provided ample evidence of fuel/cladding interaction leading to formation of low-melting phases. A large inventory of molten fuel existed at the time of fuel-pin failure; the molten fuel and a much smaller amount of fuel/steel low-melting materials were ejected upward. Only small quantities of molten material entered the plenums. The bulk of the material exited the breaches and contacted the outer surfaces of the cladding, the spacer wires, and the interior surfaces of the flowtubes. A representative cross section of the medium-burnup pin from M2 is shown in Fig. 4. Fuel/steel phases line the inner and outer surfaces of the cladding, surround the spacer wire, and coat the inner surface of the flowtube in Fig. 4(a). A higher magnification micrograph of the cladding and adherent material is shown in Fig. 4(b). Only 20% of the original cladding thickness remains as a narrow horizontal band across the center of Fig. 4(b).

The optical metallograph could not resolve the characteristic eutectic structure that should have been present in the specimen shown in Fig 4. Formation of the fuel/steel phases shown in the figure were caused by molten fuel that was well above the temperatures of formation for the two eutectics in the Fe-U system. The same specimen was examined on the scanning electron microscope in an attempt to resolve the eutectic structure and to qualitatively identify the phases present in the microstructure. A series of increasingly higher magnification secondary electron images of the specimen are shown in Fig. 5. The remaining intact cladding is shown as a black horizontal band across Fig. 5(a) and at the top of Fig. 5(b). The cladding is layered between two 25-μm-thick bands of fuel/steel material that is contacted by a region containing a fine-structured eutectic. The fine-structured fuel/steel eutectic penetrated into the boundaries around U-rich grains. Fig. 5(c) is useful to qualitatively describe the phases present in the system. The large, dark grains surrounded by a lighter phase at the top of the figure are stainless-steel-like grains surrounded by UFe_2. The fine-structured eutectic was harder to identify because of the size of the electron beam

relative to the sizes of the lamellae; however, the eutectic is probably of the type UFe_2 and Fe even though at some sites there was indication that the eutectic might be of the type U_6Fe - UFe_2. The larger grains at the bottom of Fig. 5(c) were U-rich phases containing iron and other stainless-steel constituents; however, there was no indication of original U-5Fs within any of the structures examined.

A specimen from the "dimple" region of the low-burnup pin from M2 was examined on the scanning electron microscope to determine if the cladding had been penetrated by eutectic formation. Although some eutectic was present at the fuel/cladding interface, the penetration was slight indicating that the peak temperature was below the 1350 K level thought to be needed for rapid eutectic penetration.

C. Fuel Mass Distribution, Melt Fraction, and Porosity.

In order to more fully understand the mechanisms of fuel expansion and to be able to predict its occurrence correctly, the fuel mass distribution, fuel melt fraction, and nature and distribution of porosity within intact pins from M2 and M3 were examined. Only intact pins were studied. (In the failed pins, most of the fuel was ejected from the breached cladding, and that remaining within the pin had interacted with the cladding, making it nonprototypic of prefailure fuel.)

The axial fuel mass distributions in the U-5Fs pins were evaluated by cutting and weighing short segments of measured lengths from throughout the fuel zone of each intact pin. It was assumed that the density of the cladding and amount of retained sodium within the segments were constant. The purpose of the investigation was to determine if the expanded fuel, which amounted to as much as 18% of the pretest fuel-column length, was produced from only the very top of the fuel column or if fuel from much lower contributed to the expansion. The results of the study indicated that the upper halves of the preirradiated pins contributed to the fuel expansions measured during the M2 and M3 tests. The observations were consistent for all three burnups (0.35, 4.4, and 7.9 at.% burnup). There was indication of a localized, fuel density increase just below the tops of the fuel columns. The mass/length was slightly greater there than in the remainder of the expanded fuel and less than in the lower half of the pin. This effect was most pronounced in the low-burnup pin from M2 and medium-burnup pin from M3.

The areal melt fraction (portion of the fuel cross section that experienced a peak temperature above the solidus of the U-5Fs fuel) was measured at three elevations for the intact pins from M2 and M3. The results are useful for validating codes that model fuel behavior and for planning future TREAT in-pile tests using the IFR reference ternary fuel (U-Pu-Zr). The study determined that for each of the pins all of the fuel at the as-fabricated tops of the fuel columns was above the solidus temperature. The values varied at the midplanes; the 0.35 at.% burnup pin from M2 had a melt fraction of 0.60, and the low-burnup pin from M3 had a melt fraction of slightly less than 0.60; melt fractions of 0.40 were measured for both the medium- and high-burnup pins from M3. Fuel at the bottoms of each of the fuel columns did not reach the solidus temperature.

The overall morphology and distribution of porosity varied axially and radially in a manner related to whether or not the fuel temperature exceeded the U-5Fs solidus. In addition, there seemed to be a burnup effect. The Fig. 6 micrographs show four different radial positions at the original fuel midplane in the 0.35 at.% burnup pin from test M2. The fuel/cladding gap is shown in Fig. 6(a) illustrating the overall absence of porosity in the fuel, at the right of the photograph. Figure 6(a) is representative of fuel that remained well below the solidus temperature throughout the test. The solidus isotherm nearly equally divides Fig. 6(b), with the right half representing fuel that slightly exceeded the solidus. Even though fission-gas bubbles have begun to coalesce in the left half of the photograph, that effect has only occurred at grain boundaries, and the edges of the pores are not rounded in a manner that would suggest melting. The right half of the same micrograph illustrates a significant increase in bubble coalescence, with many of the pores having smooth rounded surfaces indicative of partial melting. At the radius shown in Fig. 6(c), many of the smaller pores have further coalesced to form several much larger gas bubbles. Finally, Fig. 6(d) is indicative of fuel that has been fully liquid with nearly all of the small bubbles coalesced into bubbles so large that surface tension provides little restraint, as evidenced by deformations caused by interference with other growing bubbles. At higher elevations, large pores of the type shown in Fig. 6(d) have further coalesced to form very large single or double central bubbles.

In general, the medium- and high-burnup pins from test M3 displayed more porosity at the bottom of the fuel columns than did either of the low-burnup pins from tests M2 and M3. The pores were formed in the solid state, as illustrated in the left half of Fig. 6(b). However, above midplane the low-burnup pins contained significantly more porosity than did either of the higher burnup pins from M3.

IV. CONCLUSIONS

The results of the posttest examination of the failed and nearly-failed uranium-fissium-alloy pins from tests M2, M3, and M4 have provided a more comprehensive understanding of the mechanisms of prefailure fuel extrusion and cladding failure in metal-fuel and provide direction for study of the U-Pu-Zr IFR reference fuel alloy both in and out of pile.

V. REFERENCES

1. A. E. Wright et al, "Recent Metal Fuel Safety Tests in TREAT," Proc. of the Int'l. Conf. on Fast Reactor Safety, Guernsey, England, May 1986.

Table 1. Measured and Computed Values Pertaining to Cladding Failure and Prefailure Fuel Expansion

Test	Fuel Burnup (at.%)	Max. P/F Achieved in Test	Computed Peak Plenum Pressure[a] (MPa)	P/F at Computed Failure	Proximity to Failure (%)	Computed P/F at Onset of Fuel Melting	P/F at Half of Max. Fuel Elongation	Maximum Fuel Elongation (%)
M2	0.35	4.1	0.6-0.8	4.7	13	3.5	3.6	16
	4.4	4.2 (f)	7-9	4.5	(f)	2.7	3.8	(c)
	7.9	4.1 (f)	17-20	3.6-4.0[b]	(f)	2.7	2.9	3
M3	0.35	4.1	0.6-0.8	4.8	15	3.5	3.7	18
	4.4	4.0	7-9	4.4	5	2.5	3.1	4
	7.9	3.4	17-23	3.6-4.0[b]	17	2.5	2.5	4
M4	0.0	3.8	0.6-0.8	4.3	12	3.3	—	1
	2.4	4.1 (f)	2-6	4.4	(f)	2.3	3.2	7
	4.4	3.8	7-9	4.1	10	2.1	3.2	4

(a) The range shown reflects the uncertainty in the room-temperature pressure.
(b) Reflects the range in computed plenum pressure at failure.
(c) Data are very ambiguous but seem to suggest 10-15% elongation.
(f) Cladding failure occurred in test.

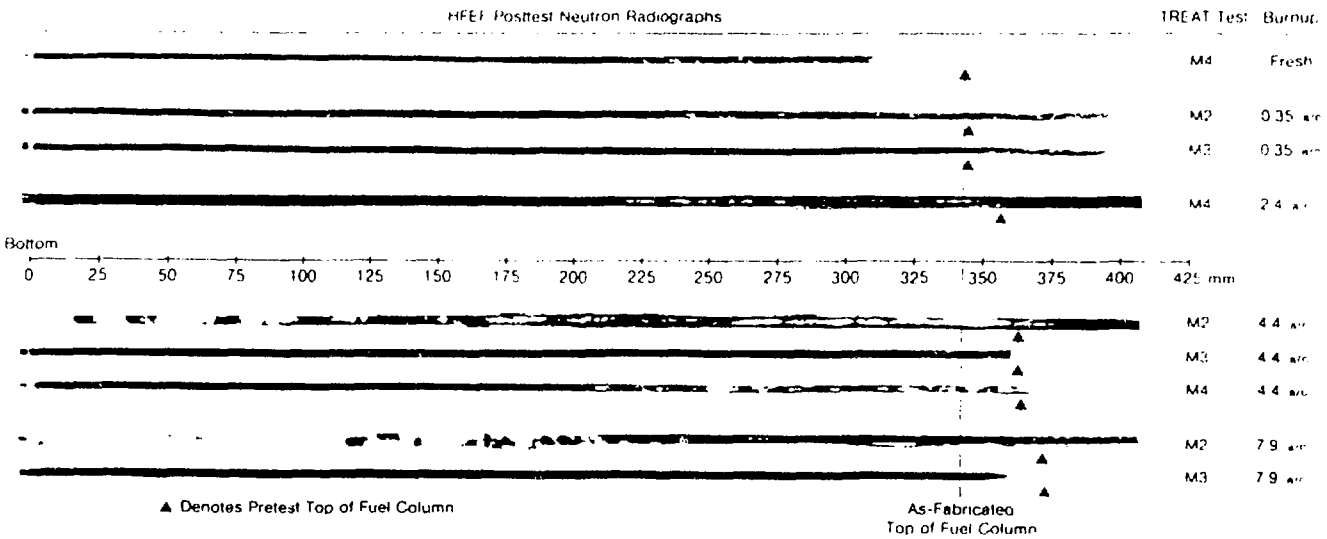

Fig. 1

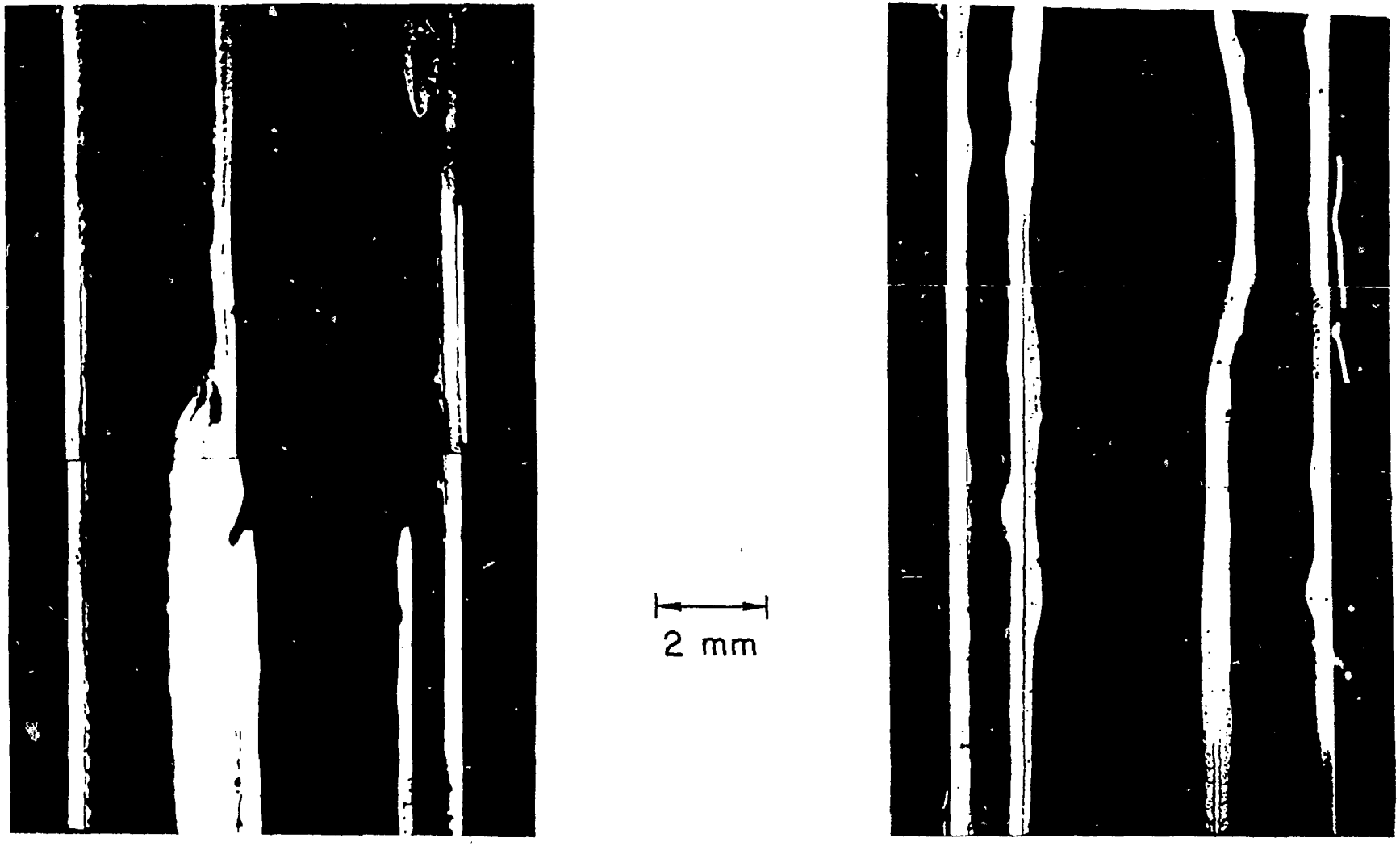

(a) 4.4 % BURNUP

(b) 7.9 % BURNUP

LONGITUDINAL SECTIONS OF U-5Fs FUEL PIN DIMPLE REGION. X/L=1.0

Fig. 2

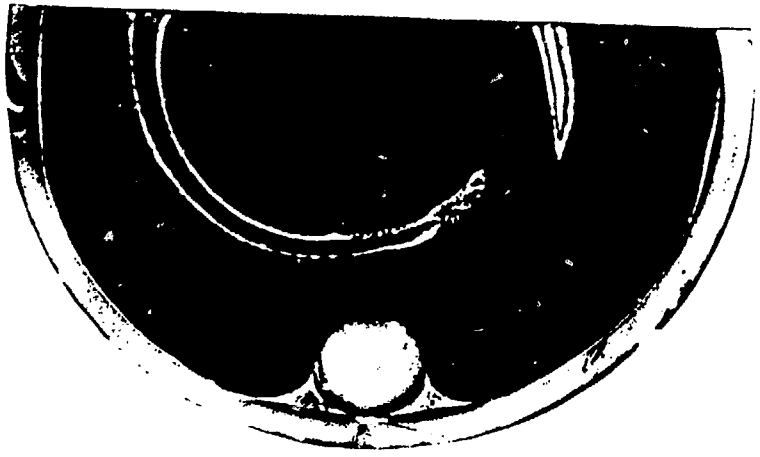

(a)

1 mm

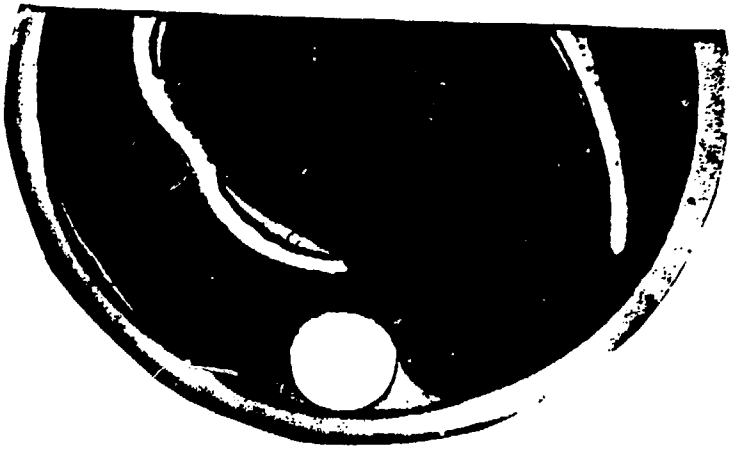

(b)

TRANSVERSE SECTION OF
7.9 % BURNUP U-5Fs
FUEL PIN. X/L = 1.0

(c)

0.5 mm

Fig. 3

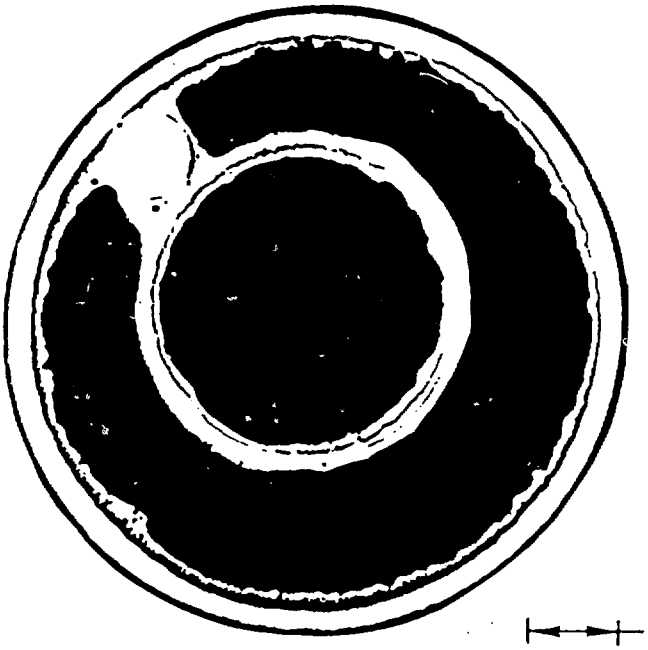

(a)

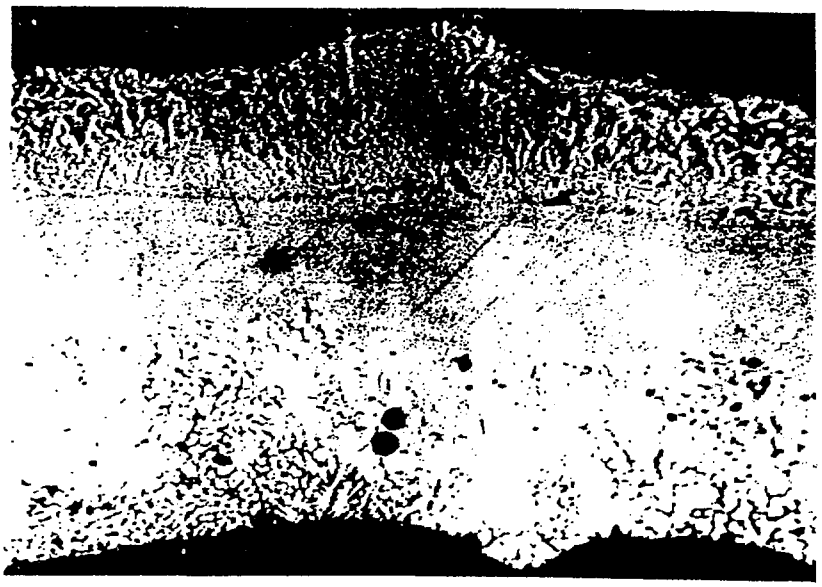

(b)

CLADDING AND FLOWTUBE OF 4.4 % BURNUP U-5Fs FUEL PIN. X/L=1.30

Fig. 4

(a) ⟷ 50 μm

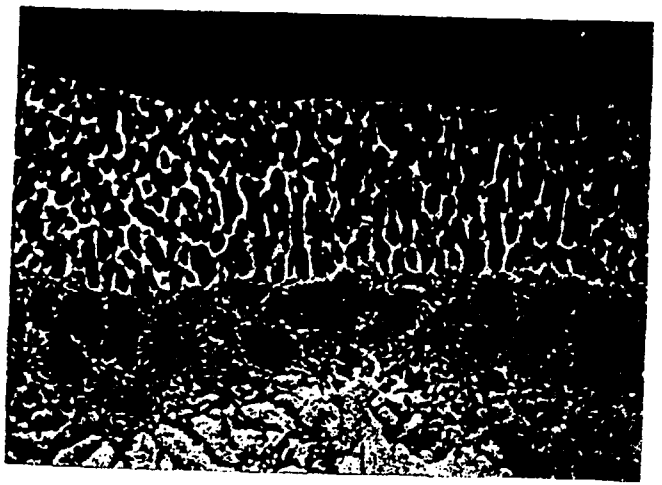

(b) ⟷ 10 μm

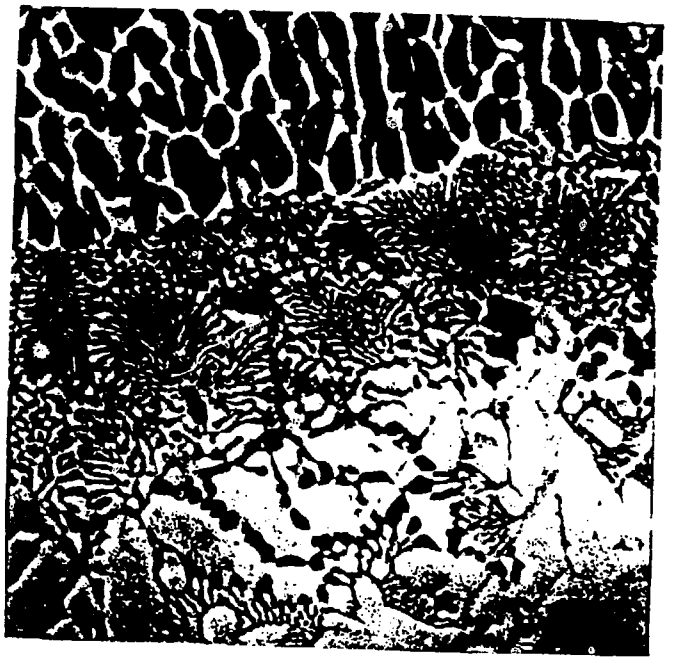

(c) ⟷ 10 μm

SECONDARY ELECTRON IMAGE
U-5Fs 4.4 % BURNUP
X/L = 1.30

Fig. 5

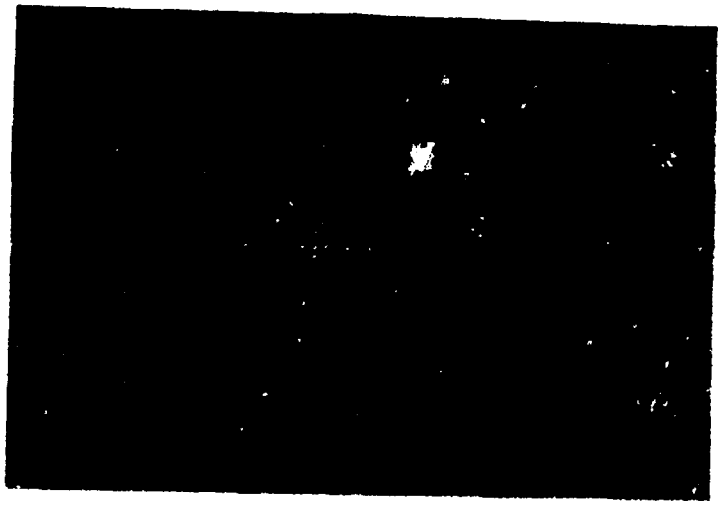

(a) $r/r_0 = 1.0$

0.1 mm

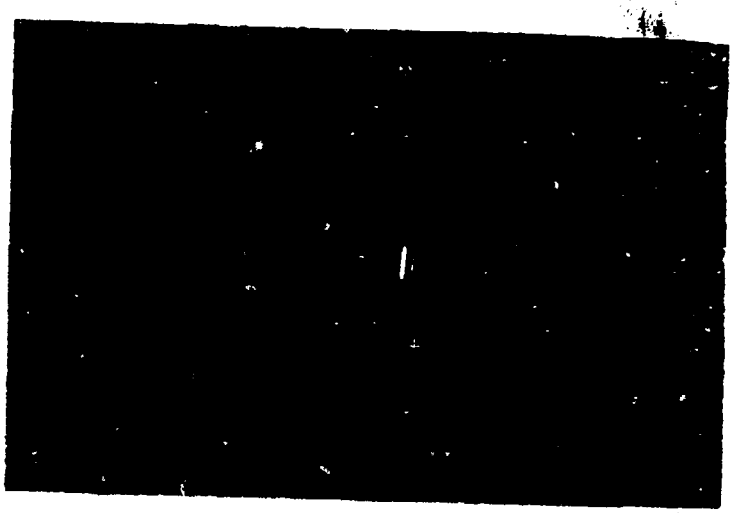

(b) $r/r_0 = 0.7$

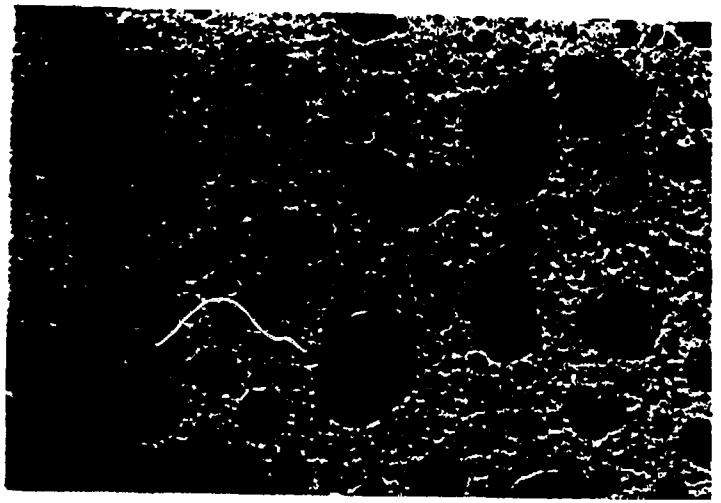

(c) $r/r_0 = 0.6$

(d) $r/r_0 = 0.3$

0.35 % BURNUP U-5Fs FUEL PIN. X/L = 0.5

Fig. 6.